# Behavior of $RuO_2$(100), (110) and (101) Single-Crystal Faces in $H_2SO_4$

**Gi-Ho Jeong**†

*Department of Chemistry, Busan National University, Busan 607, Korea*

**Hong-Lee Park**

*Department of Physics, Busan National University, Busan 607, Korea* *(Received December 31, 1981)*

The properties of $RuO_2$ (100), (101) and (110) single-crystal faces in sulfuric acid are investigated by cyclic voltammetry. The shapes of the current-voltage profiles for the (100) and (101) planes indicate mainly reversible Faradaic processes while that for the (110) face resembles that resulting from an irreversible Faradaic process.

## Introduction

Ruthenium dioxide, $RuO_2$, belongs to the family of transition-metal dioxide compounds with rutile type structure which possesses interesting electric and magnetic properties. It is well known as a corrosion-resistant low overpotential electrode for chlorine evolution[1~4]. Because of its low anodic oxygen overpotential, $RuO_2$ has been shown to be an equally effective electrode for oxygen-evolution[5~7]. Furthermore, it has recently been reported that catalytic photodecomposition of water into hydrogen and oxygen proceeds at a much higher rate when $RuO_2$ is added to $TiO_2$ electrode[8]. The latter property which is particularly significant in the case of hydrogen generation via water decomposition (either electrolysis or photoelectrolysis) becomes a part of any future energy program[9]. In addition, because of its high electric conductivity and chemical stability, $RuO_2$ shows a great promise as electrical contact material[10] and strip line conductor in integrated circuits[11]. Most of the works reported so far on the behavior of the $RuO_2$ are on the film electrodes[12~23] and very little information is available on the properties of single crystals[5]. However, data on single-crystal $RuO_2$ is highly desirable[24]. Bulk electronic band structure of single-crystal $RuO_2$ has been studied recently[25].

## Experimentals

Single crystals of $RuO_2$ of typical dimensions 6 mm×4mm ×2mm were grown in our laboratory by the method of chemical transport reaction in flowing system, a technique similar to that used by Reames[27] and Shafer[28]. The volatile $RuO_3$ is formed by the mechanism:

$$\text{Ru(solid)}+\frac{3}{2}O_2 \longrightarrow RuO_3 \text{ (gas)}$$

when atmospheric pressure of oxygen is passed over Ru metal powder at a temperature of about 1,400 °C at a flow rate of approximately 15 $cm^3$/min $RuO_3$ then decomposes and crystallizes into highly ordered single crystal of $RuO_2$ in a boat placed at a cooler temperature of about 1,000°C. Crystal faces were determined by the X-ray diffraction method to better than 1°. The (100) face was polished with 6 $\mu$m diamond paste, 12 $\mu$m alumina powder, 3 $\mu$m and 0.3 $\mu$m alumina powder and finally polish etched using Siton. The faces (101) and (110) were used as grown.

Electrical contact was established with the single crystal by attaching a flexible silver-coated copper wire to the back with silver epoxy. Crystal was then mounted in insulated support of Kel-F. Kel-F was chosen over the customary Teflon because of its better molding characteristics at 300°C in addition to its resistance to chemical attack and machinability at room temperature. Geometrical surface areas of the (100), (101) and (110) faces were 2.34, 7.15 and 3.75 $mm^2$, respectively. Unlike in the case of film electrodes where large corrections are necessary for the roughness of the surfaces[22,29] no correction was made in the present case. All potentials were measured with the reference hydrogen electrode(RHE) in the working electrolyte. The electrolyte solution was 1 *N* $H_2SO_4$ prepared from Baker Ultrex $H_2SO_4$ and triply distilled $H_2O$.

## Relults and Discussion

Current-potential curves obtained by cyclic voltammetry on the (100), (101) and (110) $RuO_2$ faces in the potential range between hydrogen and oxygen evolutions are shown in Figures 1,2 and 3, respectively. Table 1 shows the average composition and atomic density of each of the three planes. There are substantial differences among the compositions of the three planes. While only $Ru^{4+}$ ions are present on the (100) and (101) planes, both $Ru^{4+}$ and $O^{2-}$ ions constitute the (110) face. In addition, all the $Ru^{4+}$ and $O^{2-}$ ions on the planes may not be identical. For example, there are two kinds of $Ru^{4+}$ ions on the (110) surface: firstly one which needs

**TABLE 1: Atomic Characteristics of $RuO_2$ (100), (110) and (101) Crystal Planes**

| Plane | Area of the unit cell plane, $cm^2$.* | Average composition | Atomic densit (atoms/$cm^2$) | Ru–O distances |
|---|---|---|---|---|
| (100) | $14.0\times10^{-16}$ | 1 $Ru^{4+}$ | $7.1\times10^{14}$ | — |
| (101) | $24.5\times10^{-16}$ | 2 $Ru^{4+}$ | $8.2\times10^{14}$ | — |
| (110) | $19.7\times10^{-16}$ | 2 $Ru^{4+}$ | $2.0\times10^{15}$ | 1.94 Å |
| | | 2 $O^{2-}$ | | 1.98 Å |

* $a_0=b_0=4.4910$ Å, $c_0=3.1064$ Å

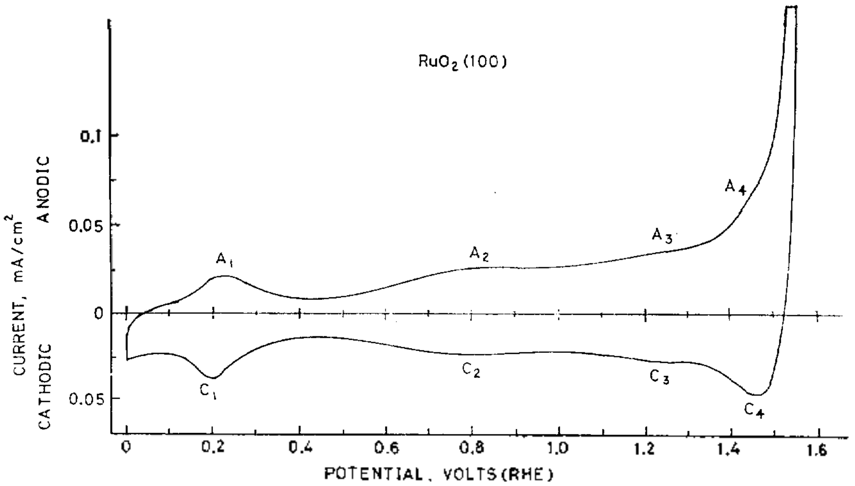

**Figure 1.** Current-potential curve obtained by cyclic voltammetry on the $RuO_2(100)$ face: scan speed=50 mV/sec.

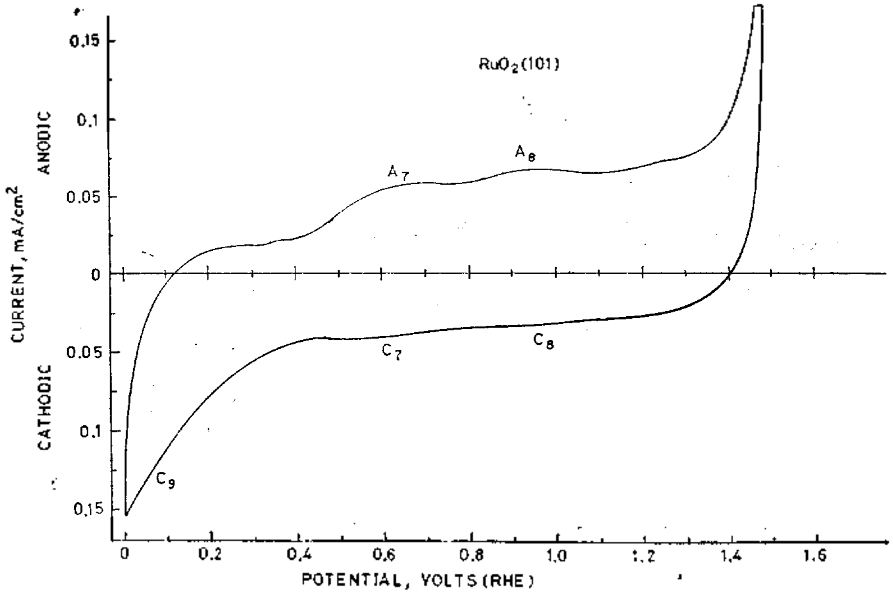

**Figure 2.** Current-potential curve obtained by cyclic voltammetry on the $RuO_2$ (101) face: scan speed=50 mV/sec.

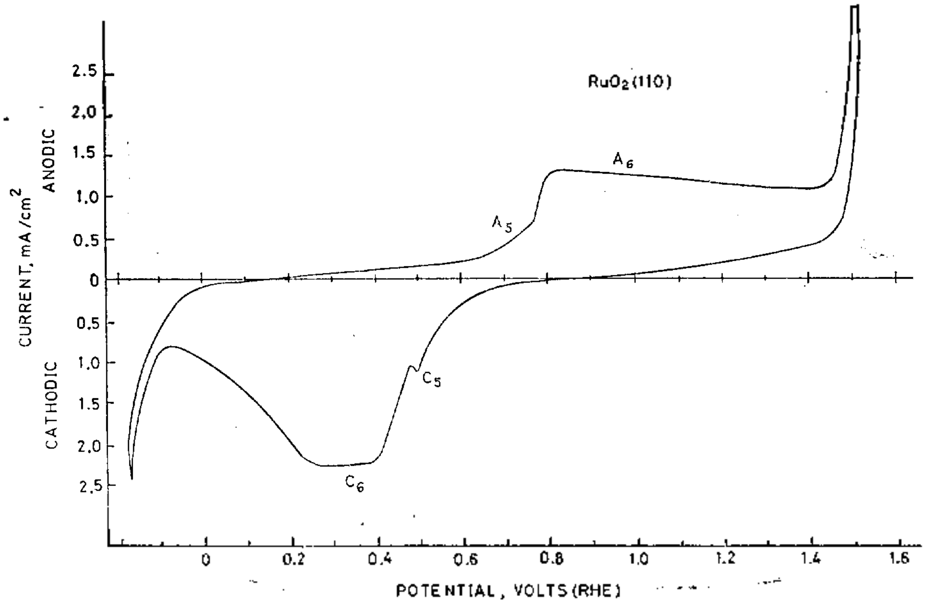

**Figure 3.** Current-potential curve obtained by cyclic voltammetry on the $RuO_2$ (110) face: scan speed=50 mV/sec.

only a single $O^{2-}$ ion per $Ru^{4+}$ ion to restore the octahedral coordination of the metal ion and the other which needs two $O^{2-}$ ions per $Ru^{4+}$ion. All the $Ru^{4+}$ ions on the (100) and on the (101) faces are alike in that they all need three more $O^{2-}$ ions to complete the octahedral symmetry of $O^{2-}$ ions around them. Planes lying just below the top plane have only $O^{2-}$ ions in every case. Cyclic voltammograms are essentially determined by the surface reactions. Bulk contributions, if any, do not seem to play a major role.

The *i*–V profiles observed in the cyclic potentiodynamic sweeps of the three crystal planes indicate different types of surface process. The shapes of the *i*–V profile for the (100) and (101) planes (Figures 1 and 2) indicate mainly reversible Faradaic processes involving surface species while that for the (110) face (Figure 3) resembles that from an irreversible Faradaic process involving deposition and electrodeposition of a surface species[30].

The *i*–V curve for the (101) surface (Figure 2) has a striking similarity to that for a $RuO_2$ film electrode[12, 21]. We observe a pair of peaks ($A_7$, $C_7$) at about 0.7 V that can be attributed to the $Ru_2O_3/Ru$ couple and another pair ($A_8$, $C_8$) at about 0.95 V which can be identified with the $Ru_2O_3/RuO_2$ couple. The former couple results in a change of oxidation state from 0 to +3 according to the reaction:

$$2Ru+3H_2O \longrightarrow Ru_2O_3+6H^++6e^-$$

while the latter takes it from +3 to +4 according to the reaction:

$$Ru_2O_3+H_2O \longrightarrow 2RuO_2+2H^++2e^-$$

The cathodic peak $C_9$ is due to the solid state reduction of $RuO_2$ accompanied by the penetration of atomic hydrgen into the lattice.

Figure 1 for the (100) plane also has a pair of peaks ($A_2$, $C_2$) at about 0.8 V which can be assigned to the $Ru_2O_3/Ru$ couple. The pair ($A_3$, $C_3$) at near 1.2 V can be accounted for by the reaction[31]:

$$Ru+4H_2O \longrightarrow RuO_4^{2-}+8H^++6e^-$$

resulting in a change of oxidation number from O to +6 though it involves the formation of a dissolvable ruthenate ion. The feature $A_4$ at about 1.4 V can be associated with the $RuO_2/RuO_4$ couple involving a change of oxidation state from +4 to +8 according to the reaction:

$$RuO_2+2H_2O \longrightarrow RuO_4+4H^++4e^-$$

Peaks at near 0.8 V and 0.7 V have also been observed for pure Ru electrodes which support our identifications of the ($A_2$, $C_2$) and ($A_7$, $C_7$) pairs with the $Ru_2O_3/Ru$ couples. The position of the peak $A_1$ at near 0.22 V was found to be unaffected by the sweep rate though its intensity decreased as the rate was increased. Furthermore, if the electrode was kept at 0 V for some time, this peak became more intense and moved to higher potentials. Thus, it can be associated with the oxidation of hydrogen atoms entrapped in the lattice.

The *i*–V curve for the (110) face (Figure 3) is characteristic of a redox process. The reason why it is far different from those on the other two faces is perhaps because there are both $Ru^{4+}$ and $O^{2-}$ ions on this plane whereas only $Ru^{4+}$ ions occupy the other two faces. The feature $A_5$ at about 0.7 V can be associated with the $Ru_2O_3/Ru$ couple and the broad peak around 0.9 V to the $Ru_2O_3/RuO_2$ couple. The break at about 0.66 V can result from a change of oxidation state from 0 to +2 at about 0.46 V followed by another change from +2 to +4 at about 1.12 V according to the reactions:

$$Ru \longrightarrow Ru^{2+}+2e^-$$
$$Ru^{2+}+2H_2O \longrightarrow RuO_2+4H^++2e^-$$

Rest potentials of the sing-crystal $RuO_2$ (100), (110) and (101) faces in 1 *N* $H_2SO_4$ have been determined to be 0.36, 0.48 and 0.69 V (RHE), respectively. On the other hand, the rest potential of $RuO_2$ film electrodes in acid soluions (1 *M* $HClO_4$) is reported to about 0.95 V (RHE)[12] which has been explained as the equilibrium potential attained after a rapid exchange of protons at the electrode–solution interface according to the reaction[31]:

$$2RuO_2+2\,H^++2e^- \longrightarrow Ru_2O_3+H_2O$$

Standard potential value of 0.43 V has been calculated[26] for the reaction:

$$RuO_2+4H^++4\,e^- \longrightarrow Ru+2H_2O$$

which is in between the values for the $RuO_2$ (100) and (110) faces. More reactions of the similar nature need to be investigated in order to explain the present results.

Oxygen evolution has been carried out on the single-crystal $RuO_2$ (100), (101) and (110) faces and Tafel slopes of 95, 115 and 105 mV/decade have been found for them. On the film electrodes, however, a Tefel slope of only 40 to 45 mV/decade has been reported[21]. These differences are not surprising in view of the stoichiometric differences between the films and single crystal planes. However, they do suggest that the mechanism of the oxygen evolution reaction are different on single-crystals than on films. Further work is in progress at this laboratoly.

## References

(1) A. T. Kuhn and C. J. Mortimer, *J. Electrochem. Soc.*, **120**, 231 (1973).

(2) S. Puschaver, *Chem. and Ind.*, 236 (1975).

(3) H. V. K. Udupa, R. Thangappan, B. R. Yadav and P. Subbian, *Chem. Age India*, **23**, 545 (1975).

(4) B. R. Dukes and R. C. Milner, *J. Electrochem. Soc.*, **117**, 9C (1970).

(5) S. Trasatti and G. Buzzanca, *J. Electroanal. Chem.*, **29**, Al (1971).

(6) W. O'Grady, C. Iwakura, J. Huang and E. Yeager, Proc. Symp. Electrocatalysis, The Electrochemical Society, Inc., Princeton, NJ, p. 286–297 (1974).

(7) L. D. Burke, O. J. Murphy, J. F. O'Neill and S. Venkatesan, *J. Chem. Soc., Faraday Trans. I*, **73**, 1,659 (1977).

(8) T. Kawai and T. Sakata, *Chem. Phys. Letters*, **72**, 1 (1980).

(9) D. P. Gregory, "Modern Aspects of Electrochemistry, "J. O'M. Bockris and B.E.Conway, Eds., Chapter 5, Plenum

Press, New York, (1975).
(10) D. J. Pedder, *Electrocomp. Sci. Tech.*, **2**, 259 (1976).
(11) M. W. Shafer and J. Armstrong, *IBM Tech. Discuss. Bull.*, **20**, No. 11A, 4,633 (1978)..
(12) D. Galizzioli, F. Tantardini and S. Trasatti, *J. Appl. Electrochem.*, **4**, 57 (1974).
(13) D. Galizzioli, F. Tantardini and S. Trasatti, *ibid.*, **5**, 203 (1975)
(14) T. Okamura, *Denki Kagatu*, **41**, 303 (1973)
(15) S. Pizzini, G. Buzzanca, C. Mari, L. Rossi and S. Torchio, *Mater. Res. Bull.* **7**, 449 (1972).
(16) G. Lodi, C. Bighi and C. de Asmundis, *Mater. Chem.*, **1**, 177 (1976).
(17) H. Tamura and C. Iwakura, *Denki Kagatu*, **43**, 674 (1975).
(18) C. Iwakura, H. Tada and H. Tamura, *Electrochim. Acta*, **22**, 217 (1977).
(19) W. A. Gerrard and B. C. H. Steele, *J. Appl. Electrochem.* **8**, 417 (1978).
(20) T. Arikado, C. Iwakura and H. Tamura, *Electrochim. Acta*, **22**, 513 (1977).
21) L. D. Burke, O. J. Murphy, J. F. O'Neill and S. Venkatesan, *J.C.S. Faraday I*, **73**, 1,659 (1977).
(22) L. Burke, O. J. Murphy and J. F. O'Neill, *J. Electroanal. Chem.* **81**, 391 (1977).
(23) G. Lodi, E. Sivieri, A. de Battiste and S. Trasatti, *J. Appl. Electrochem.* **8**, 135 (1978).
(24) S. Trasatti and W. O'Grady, Advances in Electrochemistry and Electrochemical Engineering, H. Gerischer and C. W. Tobias, eds., John Wiley and Sons, New York (1981).
(25) G. Skorinko, A. K. Goel, and F. H. Pollak, *Bull. Amer. Phys. Soc.*, **25**, 363 (1980).
(26) S. Pizzini and L. Rossi, *Z. Naturforsch.*, **26**, 177 (1971).
(27) F. M. Reames, *Mat. Res. Bull.*, **11**, 1,019 (1976).
(28) M. W. Shafer, R. A. Figat, B. Oosen, S. J. Laplace and J. Angilello, *J. Electrochem. Soc.*, **126**, 1,625 (1979).
(29) L. D. Burke and O. J. Murphy, *J. Electroanal. Chem.*, **112**, 39 (1980).
(30) H. A. Kozlowska, B. E. Conway and W. B. A. Sharp, *Electroanal. Chem. and Interfacial Electrochem.*, **43**, 9 (1973).
(31) M. Pourbaix, "Atlas of Electrochemical Equilibria in Aqueous Solutions," p. 343–349 Pergamon Press, London, 1966.

# Transition-State Variation in the Solvolysis of Benzoyl Chlorides*

**Ikchoon Lee, In Sun Koo, Se Chul Sohn and Hai Hwang Lee**

*Department of Chemistry, Inha University, Incheon 160 Korea* *(Received February 10, 1982)*

Solvolysis reactions of some substituted benzoyl chlorides were studied in ethanol-water, ethanol-trifluoroethanol and methanol-acetonitrile mixtures. Results showed that the reaction proceeds *via* an $S_N2$ process in which bond formation is more advanced than bond cleavage. Comparison of the two models for predicting transition state variation indicated superior nature of the quantum mechanical model relative to the potential energy surface model.

## Introduction

The reaction mechanism for the nucleophilic substitution reaction at a carbonyl carbon has attracted considerable attention. Specifically the mechanisms of solvolysis and nucleophilic subtitution reactions of benzoyl halides have been studied with a view to making a comparison with those of benzyl derivatives; it has been shown that both exhibit the borderline nature of the process[1], but bond-making is important in the former[1a-b] whereas in the latter bond-breaking is important[1c-d] in the transition state. Recently various models for predicting variations in transition state structure have been used in explaining the properties of nucleophilic substitution reactions. Jencks[2] discussed transition state variation with solvent using an extended Grunwald-Winstein[3] equation(1),

$$\log(k/k_0) = mY + lN \qquad (1)$$

Harris *et al.*[4] predicted variation of $S_N2$ transition state of benzyl derivatives using a potential energy surface model[5] and Lee *et al.*[6] applied the similar model to the $S_N2$ transition state of benzensulfonyl derivatives.

The potential energy surface (PES) model for predicting transition state variation is based on the application of the Hammond postulate[7] and the Thornton's rule[8] to e.g., a reaction of a nucleophile(N) attacking a substrate (RX),

$$N(B) + RX(A) \longrightarrow [N\cdots R\cdots X]^{\ddagger} \longrightarrow N^{+}-R + X^{-} \qquad (2)$$

On the other hand, Pross and Shaik[9] introduced a quantum mechanical approach to estimating the effect of subtituents on transition state structure in $S_N2$ reactions. In this model, the reaction complex is described in terms of a wave function built up from a linear combination of reactant configurations. In an $S_N2$ reaction, (2), a new bond is formed between A and B and a bond within A is borken as a substrate A(RX) is attacked by a nucleophile B(N).

---

*Taken as Part 14 of the series "Nucleophilic Substitution at a Carbonyl Carbon".